# Emissions of Carbon Tetrachloride ($CCl_4$) from Europe

Francesco Graziosi[1,2], Jgor Arduini[1,2,3], Paolo Bonasoni[3], Francesco Furlani[1,2], Umberto Giostra[1,2], Alistair J. Manning[4], Archie McCulloch[5], Simon O'Doherty[5], Peter G. Simmonds[5], Stefan Reimann[6], Martin K. Vollmer[6] and Michela Maione[1,2,3,*]

[1]Department of Pure and Applied Sciences, University of Urbino, Urbino, 61029, Italy
[2]CINFAI (National Inter-University Consortium for Physics of the Atmosphere and Hydrosphere), Rome, 00178, Italy
[3]Institute of Atmospheric Sciences and Climate, National Research Council, Bologna, 40129, Italy
[4]Hadley Centre, Met Office, Exeter, EX1 3PB, United Kingdom
[5]School of Chemistry, University of Bristol, Bristol, BS8 1TH, United Kingdom
[6]Laboratory for Air Pollution and Environmental Technology, Empa, Swiss Federal Laboratories for Materials Science and Technology, Dubendorf, 8600, Switzerland

*Correspondence to*: Michela Maione (Michela.maione@uniurb.it)

**Abstract.** Carbon tetrachloride ($CCl_4$) is a long-lived radiatively-active compound able to destroy stratospheric ozone. Due to its inclusion in the Montreal Protocol on Substances that Deplete the Ozone Layer, the last two decades have seen a sharp decrease in its large scale emissive use with a consequent decline of its atmospheric mole fractions. However, the Montreal Protocol restrictions do not apply to the use of carbon tetrachloride as feedstock for the production of other chemicals, implying the risk of fugitive emissions from the industry sector. The occurrence of such unintended emissions is suggested by a significant discrepancy between global emissions as derived by reported production and feedstock usage (bottom-up emissions), and those based on atmospheric observations (top-down emissions). In order to better constrain the atmospheric budget of carbon tetrachloride, several studies based on a combination of atmospheric observations and inverse modelling have been conducted in recent years in various regions of the world. This study is focused on the European scale and based on long-term high-frequency observations at three European sites, combined with a Bayesian inversion methodology. We estimated that average European emissions for 2006 - 2014 were 2.2 (± 0.8) Gg $yr^{-1}$, with an average decreasing trend of 6.9 % per year. Our analysis identified France as the main source of emissions over the whole study period, with an average contribution to total European emissions of approximately 26%. The inversion was also able to allow the localisation of emission "hot-spots" in the domain, with major source areas in Southern France, Central England (UK) and BE-NE-LUX (Belgium, The Netherlands, Luxembourg), where most of industrial scale production of basic organic chemicals

are located. According to our results, European emissions correspond on average to 4.0 % of global emissions for 2006-2012. Together with other regional studies, our results allow a better constraint of the global budget of carbon tetrachloride and a better quantification of the gap between top-down and bottom-up estimates.

## 1.Introduction

Carbon tetrachloride ($CCl_4$) is a near exclusively anthropogenic compound whose first uses as solvent, fire extinguisher, fumigant and rodenticide date back to 1908 (Galbally, 1976; Happell et al., 2014). The rapid increase in its production occurring between the 1950s and the 1980s is linked mainly to its use as a solvent and also to the growth in the production of chlorofluorocarbons (CFCs) made from $CCl_4$ (Simmonds et al., 1998). This led to a significant increase in the atmospheric mixing ratios of $CCl_4$, as shown by firn air analysis (Butler et al., 1999; Sturrock et al., 2002). The tropospheric lifetime, of 26 years (SPARC 2013) to 35 years (Liang et al., 2014) is the result of the sum of three partial loss rates: loss in the stratosphere (Laube et al., 2013), degradation in the ocean (Yvon-Lewis and Butler, 2002) and degradation in the soil (Happell et al., 2014).

Main concerns about this long-lived chemical are linked to its capability to destroy the stratospheric ozone layer and as a radiatively active gas, with an ozone depleting potential (ODP) of 0.72 (Harris and Wuebbles et al., 2014) and a global warming potential (GWP) of 1,730 (Myhre et al., 2013). The inclusion of $CCl_4$ in the Montreal Protocol on Substances that Deplete the Ozone Layer (MP) led to a sharp decrease in the large scale emissive use of $CCl_4$ and the consequent decline in its atmospheric mixing ratios was observed starting in the early 1990s (Fraser et al., 1994; Simmonds et al., 1998), with peak mole fractions of around 103 part per trillion (ppt) and 101 ppt in 1991 in the Northern Hemisphere (NH) and Southern Hemisphere (SH), respectively (Walker et al., 2000). In 2012 $CCl_4$ measured global average mole fractions were 84.2 and 85.1 ppt, as measured by the AGAGE (Advanced Global Atmospheric Gases Experiment) and NOAA-GMD (National Oceanic and Atmospheric Administration-Global Monitoring Division) ground-based sampling networks, respectively. The respective decrease rates during 2011-2012 were 1.2 and 1.6% $yr^{-1}$ (Carpenter and Reimann et al., 2014). The contribution of $CCl_4$ to total organic chlorine in the troposphere in 2012 was 10.3% (Carpenter and Reimann et al., 2014).

Currently, emissive uses of $CCl_4$ are banned under the MP in signatory countries. Production and use are allowed for feedstock for chemical manufacture, for example for perchloroethylene, hydrofluorocarbon (HFC) and pyrethroid pesticides production (UNEP, 2013). Chemical feedstocks should be converted into new chemicals, effectively destroying the feedstock, but fugitive emissions are possible. With no significant natural sources (Butler et al., 1999; Sturrock et al.,

2002) the possible sources for $CCl_4$ in the atmosphere are fugitive emissions from the industry sector (Simmonds et al., 1998; Fraser et al., 2014), generation during bleaching (Odabasi et al., 2014) or emissions from a legacy of $CCl_4$ in old landfill (Fraser et al., 2014).

The persistence of such emissions is suggested by a discrepancy between global emissions as derived from reported production and feedstock usage (bottom-up emissions) and those based on atmospheric observations (top-down emissions). Assuming a total atmospheric lifetime of 26 years and the observed trend in the atmosphere, the top-down global $CCl_4$ emission estimates suggest for 2011-2012 global $CCl_4$ emissions are 57 (40–74) Gg $yr^{-1}$, a value that is at least one order of magnitude higher than estimates based on industrial use (Carpenter and Reimann et al., 2014). In addition the persistence of an inter-hemispheric gradient of about 1.3 ppt (Northern Hemisphere, NH minus Southern Hemisphere, SH) since 2006, shows that $CCl_4$ is still emitted in the NH (Carpenter and Reimann et al., 2014). Similar results have been obtained by Liang et al. (2014), who deduced that the mean global emissions during 2000-2012 were 39 Gg $yr^{-1}$ (34-45 Gg $yr^{-1}$) with a calculated total atmospheric lifetime for $CCl_4$ of 35 (32-37) years.

In order to better constrain the $CCl_4$ budget, several top-down studies have been conducted in recent years focused on the global and regional scale, the top-down approach having been recognised as an important independent verification tool for bottom-up reporting (Nisbet and Weiss, 2010; Weiss and Prinn, 2011; Lunt et al., 2015).

Xiao et al. (2010) used a three-dimensional inversion model and global $CCl_4$ observations (AGAGE and NOAA-GMD) to derive emissions from eight world regions over the 1996-2004 period, identifying South-East Asia as being responsible of more than half of the global industrial emissions, which they estimated as 74.1 ± 4.3 Gg $yr^{-1}$ (9-year average).

The role of China as a significant source region of $CCl_4$ has been highlighted by Vollmer et al. (2009) who, based on 18-month continuous high-frequency observations (October 2006 – March 2008) conducted at a site in the North China Plain and a Bayesian inversion modelling approach, calculated Chinese emissions to be 15 Gg $yr^{-1}$ (10-22 Gg $yr^{-1}$) out of their global estimates of 53 ± 30 Gg $yr^{-1}$.

According to Fraser et al. (2014) top-down Australian emissions during 1996-2011 have declined from 0.25-0.35 Gg $yr^{-1}$ to 0.12-0.18 Gg $yr^{-1}$, a decline of 5% $yr^{-1}$. In this study potential sources other than those arising from production, transport and use were identified and on the basis of an analysis of pollution episodes, were likely to be associated with contaminated soils, toxic waste treatment facilities and chlor-alkali plants.

In 2012, Miller et al., used a $^{14}C$-based top-down method, to derive for the United States an average emission of 0.4 Gg $yr^{-1}$ during 2004-2009, corresponding to 4% of the global emissions given in

Montzka and Reimann et al. (2011). Emission estimates by Hu et al. (2016) during 2008-2012 were 4.0 (2.0-6.5) Gg $yr^{-1}$. This number is two orders of magnitude greater that emissions reported to the US EPA Toxic Releases Inventory over the same period and one order of magnitude larger that the previous estimates given by Miller et al. (2012). Hu et al.'s estimates were derived using observations from a large observation network including multiple sites across the United States and both a Bayesian and geostatistical inverse analyses.

For Europe, the most recent estimates are given in the above-cited paper by Xiao et al. (2010), who reported that Europe has been responsible, over 1996-2004, for 4% of global emissions. However this study, based on observations conducted at global baseline sites, did not derive regional variations that likely occur across the different European countries and that could help in identifying specific emission sources, including those unrelated to reported production.

With this aim, we conducted a study based on long-term, high-frequency $CCl_4$ observations carried out at three European sites combined with FLEXPART and the Bayesian inversion approach developed by Seibert (2000; 2001), improved by Eckhardt et al. (2008) and Stohl et al. (2009; 2010) and recently applied to derive emissions of halogenated species at the European scale (Maione et al., 2014; Graziosi et al., 2015).

Even though major source regions are likely to be located in East Asia, our results, in combination with those obtained from other regional studies, are useful in order to better assess the global budget of $CCl_4$ and better evaluate to what extent future emissions will affect the evolution of the equivalent effective stratospheric chlorine (EESC).

## 2.Method

### 2.1 Measurements

In Europe $CCl_4$ long-term, high-frequency observations of $CCl_4$ are available from three sites, all labelled as WMO-GAW (World Meteorological Organisation-Global Atmosphere Watch) global stations and AGAGE and affiliated stations: Mt. Cimone, CMN (Italy); Jungfraujoch, JFJ (Switzerland) and Mace Head, MHD (Ireland). CMN and JFJ are mountain stations occasionally affected by air masses from the polluted boundary layer; MHD baseline station is mostly affected by oceanic air masses and occasionally by air masses from over Ireland, United Kingdom and continental Europe. All $CCl_4$ data used in this paper are available from the AGAGE network: different instrumentations and protocols are used to measure in situ $CCl_4$ at each station: CMN uses a gas chromatograph with mass spectrometric detection (GC-MS), with sample enrichment on adsorbent trap by a commercial thermal desorber (Maione et al., 2013); JFJ uses a gas chromatograph with mass spectrometer detection, with sample enrichment on a custom built

thermal desorber-Medusa-GC-MS, (Miller et al., 2008); MHD uses a gas chromatograph with an electron capture detection (GC-ECD), without sample enrichment (Prinn et al., 2000). All the measurements are reported using the Scripps Institution of Oceanography (SIO), SIO-05 gravimetric primary calibration scale: ambient air measurements are routinely calibrated against whole air working standard that have been filled locally, using a bracketing technique, to override short term instrumental drifts. Working standards are then referenced on a weekly basis to tertiary tank (provided and calibrated by SIO) on site for the GC-MS measurements, i.e. CMN and JFJ. For the Mace Head GC-ECD instrument the tertiary tanks used as the working standard are prepared and calibrated at SIO at least twice, at the beginning and end of the life of the tank (Prinn et al., 2000; Miller et al., 2008). For this reason the contribution of the scale transfer (calibration) uncertainty to the total measurement uncertainty is minimized among stations, constraining the error estimate to the instrumental precision, calculated as the standard deviation (1σ) of the repeated working standard measurements for the covered period, that is typical for each site/setup and almost constant over the years of observation: CMN ± 0.39 ppt; JFJ ± 0.86 ppt and MHD ± 0.24 ppt. In addition, the analytical systems at the three stations are operated via the Linux-based chromatography software GCWerks (gcwerks.com) developed within the AGAGE programme.

### 2.2 Inverse modelling

Observations have been combined with 20-day backward trajectories of the FLEXPART Lagrangian Particle Dispersion Model (Stohl et al., 2005). FLEXPART runs are based on the European Centre for Medium-range Weather Forecast (ECMWF) wind fields, using 3-hourly ECMWF Re-Analyses, (ERA-Interim) (analysis fields are at 00:00, 06:00, 12:00 and 18:00 UTC, and 3-h forecasts are at 03:00, 09:00, 15:00 and 21:00 UTC) with 1°x1° horizontal resolution and 91 vertical levels. The emission sensitivity map of source-receptor relationships (SRR) generated using the three European stations is reported in Fig.1. The obtained SRR combined with an *a priori* emission field allowed us to estimate the *a posteriori* emission flux for the European Geographic Domain (EGD), using the Bayesian inversion technique.

With the aim of obtaining the best performance of the model in terms of the correlation coefficient between the observations and the modelled time series, we tested seven *a priori* emission fields based on different combinations of: i) $CCl_4$ emission fluxes estimated by Xiao et al. (2010), ii) $CCl_4$ emissions in the European Pollutant Release and Transfer Register (E-PRTR, http://prtr.ec.europa.eu/#/home), reporting $CCl_4$ atmospheric emissions higher than 100 kg $yr^{-1}$ from 30,000 industrial facilities in the domain from 2007 to 2013, iii) information on the potential chlorine production from chlor-alkali plants as in the Eurochlor report (www.eurochlor.org), providing information on the chlorine potential production of each plant from 2006 to 2014 iv) $CCl_4$

emission factors from the chlor-alkali industry derived by Brinkmann et al. (2014) and Fraser et al. (2014), and v) diffusive emissions from the use of bleach containing cleaning agents (Odabasi et al., 2014). In the seven *a priori* emission fields tested the parameterisation range was: i) from 0.6 to 4.4 Gg $yr^{-1}$ for the total *a priori* emission flux from the EGD, ii) from 3% to 80% for the contribution of industrial activities to the total EGD flux and iii) from 0.03 to 0.4 kg $CCl_4$ for each tonne of chlorine produced by the chlor-alkali plants listed in Eurochlor.

Despite these large ranges of values, the resulting EGD emission fluxes converged to very similar values, well within the inversion uncertainty, confirming the robustness of the method. For this study we used an "Ensemble" a priori emission field that showed the best model performance. The detailed description of the tests performed is reported in the Supplementary Material.

The inversion grid consists of more than 5.000 grid boxes with different horizontal resolution ranging from 0.5° by 0.5° to 2.0° by 2.0° latitude-longitude in order to assure similar weight on the inversion result. We estimated nine years of European emissions, from January 2006 to December 2014. From January 2006 to December 2014 the inversion was run using the only two stations (CMN and MHD) in which observations were available. During 2010-2014, data from JFJ were also used. A detailed description of the inversion technique and of the related uncertainty is given in the Supplementary Material.

## 3. Results and discussion.

### 3.1 Time Series Statistical Analysis

$CCl_4$ time series at three European stations are reported in Fig. 2. Using a statistical approach described in Giostra et al. (2011) we discriminate background mole fractions (black dots) from elevations above the baseline (red dots) due to pollution episodes. The monthly mean background mole fractions have been used to derive $CCl_4$ atmospheric trends, applying the empirical model described in Simmonds et al. (2004). Atmospheric trends in the background mole fractions over the common period (July 2010- Dec 2014) are -1.5±0.2, -1.2±0.1, -1.3±0.1% $yr^{-1}$ ($R^2$ = 0.93, 0.99, 0.98), at CMN, MHD, and JFJ, respectively. Such values are consistent with global trends given in Carpenter and Reimann et al. (2014).

### 3.2 Inversion Results

$CCl_4$ emission intensity from the EGD and the emission distribution within the same domain has been estimated using the European observations and the described Bayesian inversion technique. As shown in Figure 3, the main deviations between our estimates (flux $_{post}$) and the *a priori* values (flux $_{prior}$) are found in 2006, and in 2013-2014. The relative percentage bias, given by (flux $_{post}$ – flux

$_{prior}$)/flux $_{prior}$ *100), ranges from + 15% to -37%, as shown in the bottom panel of Fig 3. The emission flux uncertainty decreases from 180% of the *a priori* to 33% of the *a posteriori* emission field (average over the study period), supporting the reliability of the results. More details on the method performance are given in the Supplementary Material.

### 3.2.1 European emissions and emission trends

The inversion results indicate average EGD emissions during the study period of 2.2 (± 0.8) Gg yr$^{-1}$. $CCl_4$ total emissions from the EGD have decreased from ~ 2.8 (± 1.0) Gg yr$^{-1}$ in 2006 to ~ 1.5 (± 0.5) Gg yr$^{-1}$ in 2014, corresponding to an average EGD decreasing trend of 6.9 % per year (Figure 4). To put European emissions in a global perspective, we compared our results with global estimates. Global top-down emissions as derived from atmospheric measurements are available only until 2012 (Carpenter and Reimann et al., 2014). For the sake of consistency, this comparison was made considering the same time period, when we estimated EGD average emissions of 2.5 Gg yr$^{-1}$, corresponding to 4% of the global average. The plot in Fig.4 also shows a comparison between the EGD and the global emission trends. Over 2006-2012, the EGD estimates show an average trend -2.9% yr$^{-1}$ compared with a global trend, for the same period, of -2.2% yr$^{-1}$. For comparison, during 2004-2011 the decreasing trend in Australian emissions was 5% yr$^{-1}$ (Fraser et al., 2014).

EGD and macro-areas emission estimates for the single years are given in Table I. Such figures cannot be reconciled with potential emissions estimated from European production data reported to UNEP that, along the study period with exception of 2012, are negative, being calculated as the amount of controlled substances produced, minus the amount destroyed and the amount entirely used as feedstock. The discrepancy between the inversion results and the emissions reported to UNEP by industry persists also if a 2% of fugitive emissions and a 75% of destruction efficiency are hypothesised. (UNEP Production database, http://ozone.unep.org/). Also when comparing our estimates with emissions from the industrial activities declared to the E-PRTR, we found the latter to be strongly (on average 35 times) under-estimated, reinforcing the incompleteness of available information.

### 3.2.2 Emission distribution within the domain and emission hot spots

The obtained EGD *a posteriori* emission fluxes differ from the *a priori* both in intensity (as described above) and in spatial distribution.

In order to quantitatively assess the contribution to the total European emissions of $CCl_4$ from the various countries, we have divided our domain into ten macro areas (acronyms given in Table 1), whose extension is related to the SRR of the area (see Figure 1). Emissions from the single macro

areas and the associated uncertainty (see Supplementary Material) are reported in Table 1 and in Figure 5a. Figure 5b shows the percentage contribution from the single macro areas.

Our estimates identify FR as the main emitter in the EGD over the entire study period, with an average contribution of approximately 26%. Six macro areas (ES-PT > NEE > DE-AT > SEE> UK-IE > IT) contribute between 13.2 and 7.6%, while the remaining regional contributions average 4% each. Emissions from France reached a maximum in 2010. Emissions from IT and CH show a faster decreasing trend with respect to the average EGD rate and the remaining macro areas decreased according to the overall average EGD emissions. As a result, starting from 2008, the percent contribution of France is about the 30 % of total EGD emissions.

Beside the overall picture given by the analysis of the aggregated macro area emission estimates, the analysis of the spatial distribution of the emission fluxes provides additional insights. The map in Figure 6 shows the *a posteriori* average distribution of emission fluxes over the study period, obtained with the "Ensemble" *a priori* emission field.

The geo-referenced emission sources as reported by the E-PRTR inventory, open circles, with the dimension of the circles referring to the amount released are shown. Crosses refer to the geo-referenced Eurochlor chlor-alkali plants, for which the information on $CCl_4$ fluxes is not available.

Figure 6 shows how, in general, the localisation of the main emission sources declared by E-PRTR is well captured by the inversion, as in the case of Southern France, Central England (UK) and BE-NE-LUX. In addition, many hot spots are coincident with the chlor-alkali industries reported in Eurochlor, see e.g. the Bavarian region in Southern Germany, Sardinia (Italy) and Southern Spain. These hot spots are observed even when the inversion is run using the *a priori* emission field that does not include the E-PRTR and/or Eurochlor information on industrial emissions (not shown), indicating that the emission hot spots are not forced by the *a priori* flux.

In order to facilitate the comprehension of the map in Fig. 6, we compared the E-PRTR emission fluxes with estimates from the grid cells included in the corresponding hot spot areas identified through the inversion. We found that emission fluxes for the hot spots in Southern France and Central England were one order of magnitude larger than the reported ones and for BE-NE-LUX emissions were five times larger than those declared in the E-PRTR inventory. These results suggest either an under-reporting of current emissions and/or the occurrence of additional sources not reported by the E-PRTR inventory and/or emissions from the chlor-alkali industry and/or from historical production (such as landfill) (Fraser et al., 2014).

### 3.2.3 Comparison with NAME

For comparison, we ran an alternative top down approach based on observations at MHD combined with the UK MetOffice Numerical Atmospheric dispersion Modelling Environment (NAME) to

simulate the dispersion and an iterative best fit technique (the simulated annealing) to derive regional emission estimates (Manning et al., 2011). This alternative top-down approach differs from our procedure in the dispersion model, in the inversion technique, in the absence of an *a priori* emission field and in the use of a single receptor. The use of a single station narrows the study area to a sub-EGD that includes eight countries in North West Europe (NWEU), i.e. BE-NE-LUX, DE, DK, FR, IE and UK. Figure 7 reports a comparison of the results obtained using the two different approaches for UK only and for the NWEU domain. Overall, a fair agreement is observed, with the differences between the two estimates always within the emission uncertainty. Such encouraging results endorse the reliability of the estimated emissions.

### 3.3 Industrial emission factors

UNEP (2009) identified chlor-alkali plants as potential accidental sources of $CCl_4$. Consistently, in the U.S., Hu et al. (2016) reported emission hot-spots in areas where chlor-alkali plants are located. In addition, Fraser et al. (2014) suggest that plants based on the out dated Hg cells technology could be the main responsible for $CCl_4$ emissions. In Europe, the last two decades have seen efficient improvements in the chlor-alkali production technologies and Brinkmann et al. (2014) estimated an emission factor (EF) of 0.03 kg $CCl_4$ tonne$^{-1}$Cl. From our estimates we derived an average EF from the EGD of 0.21 kg $CCl_4$ tonne$^{-1}$Cl produced during 2010-2014 that, as shown in paragraph 3.2.2, follows the distribution of industrial plants. These figures can be compared against a value of 0.39 calculated (Fraser, personal communication) for 2008-2011 on the base of U.S. emission estimates given by Hu et al. (2016), and a value of 0.41 for 2004-2011, based on Australian emissions (Fraser et al., 2014). Indications on the reasons of discrepancies between our EF and that given by Brinkmann et al. (2014) and between our EF and that calculated for U.S. and Australia, could be provided by an analysis at the macro area level. Our estimates show how the emission factors are not homogeneous across the macro areas in the EGD, with DE-AT, BE-NE-LUX and SCA exhibiting EFs of the same order of magnitude of those given in Brinkmann et al., whereas values for the remaining macro areas are one order of magnitude higher. Indeed, $CCl_4$ emission fluxes estimated for the different macro areas of the EGD (reported in Figure 5), even after subtraction of the diffuse share (following the population density), are not directly related to the chlorine potential production in the same macro-areas (Eurochlor, 2014; for further details see Figure 6S, in the Supplementary Material). A reason of this lack of correlation could be ascribable to the inhomogeneous penetration of the different technologies in the various EGD macro areas (Eurochlor, 2014; for further details see Figure 7S, in the Supplementary Material), suggesting that $CCl_4$ fluxes are more related to the adopted technology rather than to the amount of chlorine produced. The determination of such emission rates is made even more difficult by additional

factors, like i.e. lack of obligation, for the chlor-alkali plants allowed to use $CCl_4$ as process agent for the elimination of nitrogen trichloride and the recovery of chlorine from tail gases, to report the actual amount used and/or the transfer of the allocated quota (Brinkmann et al., 2014).

## 4. Conclusions

In this study we have estimated European emissions of carbon tetrachloride combining atmospheric observations at three European sites with a Lagrangian dispersion model (FLEXPART) and a Bayesian inversion method. This procedure allowed us to assess the $CCl_4$ emission field with a high spatial resolution within the domain.

We estimated average emissions from the European Geographic Domain during 2006-2014 of 2.2 (± 0.8) Gg $yr^{-1}$, with a decreasing rate of 6.9% per year. Such an emission flux corresponds to the 4% of the global emissions estimates given by Carpenter and Reimann et al. (2014) over the period 2006-2012.

When comparing emissions derived with the top-down approach with those evaluated through bottom-up methods, large discrepancies are observed. Such discrepancies are expected with regard to the information contained in the UNEP database, which reports production (without allowing for stock change but quoting destruction as a negative production) and consumption for emissive uses. Also emissions reported in the E-PRTR inventory, that should include data related to those industrial processes (including waste treatment) that can potentially emit $CCl_4$, represent only about 3% of our estimates. However, in spite of the discrepancy in the quantification of emissions, the inversion is able to localise the main source areas reported in the E-PRTR. In addition, we note that many areas where chlor-alkali plants are located are identified as source areas by the inversion, even when the information related to such plants is not included in the *a priori* emission field. Thus, the estimated *a posteriori* emission flux seems to confirm that chlor-alkali plants are mainly responsible for $CCl_4$ emissions in the domain (UNEP, 2009).

We have also calculated the rate of $CCl_4$ emitted into the atmosphere per amount of chlorine produced in the chlor-alkali industry obtaining an average emission factor for Europe of 0.21 kg $CCl_4$ $tonne^{-1}$Chlorine produced. This value is lower than those for the U.S. (0.39) and Australian (0.41) plants. This European average emission factor includes a high variability across the various macro areas in the domain, showing the inadequacy of the chlorine potential production as a proxy of $CCl_4$ emissions as well as the relevance of the chlorine production technologies adopted by the chlor-alkali industry (including the direct use of $CCl_4$ to abate nitrogen trichloride emissions).

To summarize, this study allowed us to estimate $CCl_4$ emission fluxes at the European regional scale. Thanks to the good sensitivity in most of the EGD, the emission field can be reconstructed with a resolution level able to show, for each country, the main inconsistencies between the national emission declarations and the estimates based on atmospheric observations. Our results could allow a better constraint of the global budget of $CCl_4$ and a better quantification of the gap between top-down and bottom-up estimates, even if our estimates together with those derived by other regional studies (Fraser et al., 2014; Hu et al., 2016; Vollmer et al., 2009) still do not add up to the total amount required to comply with the current atmospheric abundance as in Carpenter and Reimann (2014). Such a discrepancy can be ascribed either to missing sources or to a lack of data from un-sampled regions of the world or to an incorrect evaluation of $CCl_4$ atmospheric lifetime, as recently shown in a study by Butler et al. (2016), whose reconsideration of $CCl_4$ total lifetime could contribute to narrowing the gap between top-down and bottom-up estimates.

***Acknowledgements.*** We acknowledge the AGAGE science team as well as the station personnel for their support in conducting in situ measurements. Measurements at Jungfraujoch are supported by the Swiss Federal Office for the Environment (FOEN) through the project HALCLIM and by the International Foundation High Altitude Research Stations Jungfraujoch and Gornergrat (HFSJG). Measurements at Mace Head are supported by the Department of the Energy and Climate Change (DECC, UK) (contract GA0201 to the University of Bristol). The InGOS EU FP7 Infrastructure project (grant agreement n° 284274) also supported the observation and calibration activities. The University Consortium CINFAI (Consorzio Interuniversitario Nazionale per la Fisica delle Atmosfere e delle Idrosfere) supported F. Graziosi grant (RITMARE Flagship Project). The "O. Vittori" station is supported by the National Research Council of Italy.

**References**

Brinkmann, T., Giner Santonja, G., Schorcht, F., Roudier, S., Delgado Sancho, L.: Industrial Emissions Directive 2010/75/EU, Integrated Pollution Prevention and Control, Science and Policy Reports. Best Available Techniques (BAT). Reference Document for the Production of Chlor-alkali. EC-JRC, Joint Research Centre of the European Commission, Luxembourg: Publications Office of the European Union, 2014.

Butler, J. H., Battle, M., Bender, M. L., Montzka, S. A., Clarke, A. D., Saltzman, E. S., Sucher, C. M., Severinghaus, J. P., and Elkins, J. W.: A record of atmospheric halocarbons during the twentieth century from polar firn air, Nature, 399, 749 – 755, 1999.

Butler, J.H., Yvon-Lewis, S.A., Lobert, J.M., King, D.B., Montzka, S.A., Bullister, J.L., Koropalov, V., Elkins, J.W., Hall, B.D., Hu, L. and Liu, Y.: A comprehensive estimate for loss of atmospheric carbon tetrachloride ($CCl_4$) to the ocean. Atmos. Chem. Phys. Discuss., doi:10.5194/acp-2016-311, in review, 2016.

Carpenter, L.J. and Reimann, S. (Lead Authors), Burkholder, J.B., Clerbaux, C., Hall, B.D., Hossaini, R., Laube, J.C., and S.A. Yvon-Lewis: Ozone-Depleting Substances (ODSs) and Other Gases of Interest to the Montreal Protocol, Chapter 1 in Scientific Assessment of Ozone Depletion: 2014, Global Ozone Research and Monitoring Project – Report No. 55, World Meteorological Organization, Geneva, Switzerland, 2014.

Eckhardt, S., Prata, A. J., Seibert, P., Stebel, K., and Stohl, A.: Estimation of the vertical profile of sulfur dioxide injection into the atmosphere by a volcanic eruption using satellite column measurements and inverse transport modelling, Atmos. Chem. and Phys. 8, 3881–3897, 2008.

Fraser, P., Gunson, M., Penkett, S., Rowland, F. S., Schmidt, U., and Weiss, R.: Report on concentrations, lifetimes, and trends of CFCs, halons, and related species, NASA Ref Publ., 1339, 1.1-1.68, 1994

Fraser, P., Krummel, P., Dunse, B., Steele, P., Derek, N., Allison, C.: Global and Australian emissions of ozone depleting substances, DSEWPaC research projects 2010–11, Australian Government Department of Sustainability, Environment, Water, Population and Communities, CSIRO and the Australian Bureau of Meteorology, ISBN: 978-1-921733-56-7, 2011

Fraser, P., Dunse, B., Manning, A. J., Wang, R., Krummel, P., Steele, P., Porter, L., Allison, C., O'Doherty, S., Simmonds, P., Mühle, J., and Prinn, R.: Australian carbon tetrachloride ($CCl_4$) emissions in a global context, Environ. Chem., 11, 77–88, 2014.

Galbally, I. E., Man-Made Carbon Tetrachloride in the Atmosphere, Science, 193/4253, 573-576, doi: 10.1126/science.193.4253.573, 1976.

Giostra U., Furlani F., Arduini J., Cava D., Manning A.J., O'Doherty S. J., Reimann S., Maione M.: The determination of a regional atmospheric background mixing ratio for anthropogenic

greenhouse gases: a comparison of two independent methods, Atmos. Environ., 45, 7396-7405,2011

Graziosi, F., Arduini, J., Furlani, F., Giostra, U., Kuijpers, L. J. M., Montzka, S. A., Miller, B. R., O'Doherty, S. J., Stohl, A., Bonasoni, P., and Maione, M.: European emissions of HCFC-22 based on eleven years of high frequency atmospheric measurements and a Bayesian inversion method, Atmos. Environ., 112, 196, 2015.

Harris, N. R. P., Wuebbles, D. J., Daniel, J. S., Hu, J., & Kuijpers, L.J.M., Law, K.S., Prather, M.J., and Schofield, R.: Scenarios and Information for Policymakers, Chapter 5 in Scientific Assessment of Ozone Depletion: 2014, Global Ozone Research and Monitoring Project-Report No. 55. World Meteorological Organization, Geneva, Switzerland, 2014.

Happell J. D., Mendoza Y., Goodwin K.: A reassessment of the soil sink for atmospheric carbon tetrachloride based upon static flux chamber measurements, J. Atmos. Chem., 71, 113-123, 2014.

Hu, L., Montzka, S. A., Miller, B. R., Andrews, A. E., Miller J. B., Lehman, S. J., Sweeney, C., Miller S., Thoning, K., Siso, C., Atlas, E., Blake, D., de Gouw, J. A., Gilman, J. B., Dutton, G.J., Elkins, J. W., Hall, B. D., Chen, H., Fischer, M. L., Mountain, M., Nehrkorn, T., Biraud, S. C., Moore, F. and Tans, P. P.: Continued emissions of carbon tetrachloride from the U.S. nearly two decades after its phase-out for dispersive uses, P. Natl. Acad. Sci. USA, 113, 2880-2885, 2016.

Laube, J. C., Keil, A., Bönisch, H., Engel, A., Röckmann, T., Volk, C. M., and Sturges, W. T.: Observation-based assessment of stratospheric fractional release, lifetimes, and ozone depletion potentials of ten important source gases, Atmos. Chem. Phys., 13, 2779-2791, doi:10.5194/acp-13-2779-2013, 2013.

Liang, Q., Newman, P.A., Daniel, J. S., Reimann, S., Hall, B. D., Dutton, G., Kuijpers, L. J. M.: Constraining the carbon tetrachloride ($CCl_4$) budget using its global trend and inter‐hemispheric gradient, Geophys. Res. Lett., 41, 5307-5315, doi: 10.1002/2014GL060754, 2014.

Lunt M.F., M. Rigby , A. L. Ganesan , A. J. Manning , R. G. Prinn , S. O'Doherty , J. Muhle , C. M. Harth , P. K. Salameh , T. Arnold , R. F. Weiss , T. Saito , Y. Yokouchi , P. B. Krummel , L. Steele, P. J. Fraser , S. Li , S. Park , S. Reimann , M. K. Vollmer , C. Lunder , O. Hermansen ,

N.Schmidbauer , M. Maione , J. Arduini , D. Young , P. G .Simmonds: Reconciling reported and unreported HFC emissions with atmospheric observations, P. Natl. Acad. Sci. USA, 112, 5927-5931 doi:10.1073/pnas.14202471122015, 2015.

Maione M., Giostra U., Arduini J., Furlani F., Graziosi F., Lo Vullo E., Bonasoni P.,: Ten years of continuous observations of stratospheric ozone depleting gases at Monte Cimone (Italy) - Comments on the effectiveness of the Montreal Protocol from a regional perspective, Sci. Total Environ. 445–446, 155–164, 2013.

Maione M., Graziosi, F., Arduini, J., Furlani, F., Giostra, U., Blake, D.R., Bonasoni, P., Fang, X., Montzka, S.A., O'Doherty, S.J., Reimann, S., Stohl, A., and Vollmer, M.K.: Estimates of European emissions of methyl chloroform using a Bayesian inversion method, Atmos. Chem. and Phys. 14, 9755-9770, doi:10.5194/acp-14-9755-2014, 2014.

Manning, A. J., O'Doherty, S., Jones, A. R., Simmonds, P. G., and R. G. Derwent: Estimating UK methane and nitrous oxide emissions from 1990 to 2007 using an inversion modelling approach, J. Geophys. Res., 116, D02305, doi:10.1029/2010JD014763, 2011.

Miller B.R., Weiss R.F., Salameh P.K., Tanhua T., Greally B.R., Mühle J., Simmonds P.G.: Medusa: A sample preconcentration and GC/MS detector system for in situ measurements of atmospheric trace halocarbons, hydrocarbons, and sulphur compounds, Anal. Chem., 80, 1536-1545, 2008.

Miller, J.B., Lehman, S.J., Montzka, S.A., Sweeney, C., Miller, B.R., Karion, A., Wolak, C., Dlugokencky, E.J., Southon, J., Turnbull, J.C., and Tans, P.P.: Linking emissions of fossil fuel $CO_2$ and other anthropogenic trace gases using atmospheric 14 $CO_2$ , J. Geophys. Res., 117 D08302, doi: 10.1029/2011JD017048, 2012.

Montzka, S.A., and Reimann, S. (Coordinating Lead Authors), Engel, A., Krüger, K., O'Doherty, S., Sturges, W.T., Blake, D.R., Dorf, M., Fraser, P.J., Froidevaux, L., Jucks, K., Kreher, K., Kurylo, M.J., Mellouki,A., Miller, J., Nielsen, O.-J., Orkin, V.L., Prinn, R.G., Rhew, R., Santee, M.L., and Verdonik D.P: Ozone-Depleting Substances (ODSs) and related chemicals, Chapter 1 in Scientific Assessment of Ozone Depletion: 2010, Global Ozone Research and Monitoring Project—Report No. 52, World Meteorogical Organization, Geneva, Switzerland, 2011.

Myhre, G., Shindell, D., Bréon, F.-M., Collins, W., Fuglestvedt, J., Huang, J., Koch, D., Lamarque, J.-F., Lee, D., Mendoza, B., Nakajima, T., Robock, A., Stephens, G., Takemura, T. and Zhang, H.: Anthropogenic and Natural Radiative Forcing. In: Climate Change 2013: The Physical Science Basis. Contribution of Working Group I to the Fifth Assessment Report of the Intergovernmental Panel on Climate Change [Stocker, T.F., Qin, D., Plattner, G.-K., Tignor, M., Allen, S.K., Boschung, J., Nauels, A., Xia, Y., Bex, V. and Midgley, P.M. (eds.)]. Cambridge University Press, Cambridge, United Kingdom and New York, NY, USA, 2013.

Nisbet, E., and Weiss, R.: Top-Down Versus Bottom-Up, Science, 328, 1241-1243, doi:10.1126/science.1189936, 2010.

Odabasi, M., Elbir, T., Dumanoglu, Y., Sofuoglu, S.C.: Halogenated volatile organic compounds in chlorine-bleach-containing household products and implications for their use. Atmos. Environ. 92, 376-383, 2014.

Prinn, R. G., Weiss, R. F., Fraser, P. J., Simmonds, P. G., Cunnold, D. M., Alyea, F. N., O'Doherty, S., Salameh, P., Miller, B. R., Huang, J.,Wang, R. H. J., Hartley, D. E., Harth, C., Steele, L. P., Sturrock, G., Midgley, P. M., and , A.: A history of chemically and radiatively important gases in air deduced from ALE/GAGE/AGAGE, J. Geophys. Res., 105, 17751–17792, 2000.

Seibert, P.: Inverse modelling of sulphur emissions in Europe based on trajectories, in: Inverse Methods in Global Biogeochemical Cycles, edited by: Kasibhatla, P., Heimann, M., Rayner, P., Mahowald, N., Prinn, R. G., and Hartley, D. E., 147–154, Geophysical Monograph, 114, American Geophysical Union, ISBN:0-87590-097-6, 2000.

Seibert, P.: Inverse modelling with a Lagrangian particle dispersion model: application to point releases over limited time intervals, In: Air Pollution Modelling and its Application XIV, edited by: Schiermeier F. A., and Gryning S.-E., Kluwer Academic Publ., 381–389, 2001.

Simmonds, P. G., Cunnold, D. M., Weiss, R. F., Prinn, R. G., Fraser, P. J., McCulloch, A., Alyea, F. N., and O'Doherty, S.: Global trends and emissions estimates of $CCl_4$ from in-situ background observations from July 1978 to June 1996, J. Geophys. Res., 103, 16,017–16,027, 1998.

Simmonds, P.G., O'Doherty, S., Derwent, R.G., Manning, A.J., Ryall, D.B., Fraser, P., Porter, L., Krummel, P., Weiss, R., Miller, B., Salameh, P., Cunnold, D., Wang, R., Prinn, R.: AGAGE observations of methyl bromide and methyl chloride at the Mace Head, Ireland and Cape Grim, Tasmania, 1998-2001, J. Atmos. Chem., 47, 3, 243-269, 2004.

SPARC, SPARC Report on the Lifetimes of Stratospheric Ozone-Depleting Substances, Their Replacements, and Related Species, Ko, M., Newman, P., Reimann, S., and Strahan, S. (Eds.): SPARC Report No. 6, WCRP-15/2013 (http://www.sparc-climate.org/publications/sparc-reports/sparc-report-no6/), 2013.

Stohl, A., Forster, C., Frank, A., Seibert, P., and Wotawa, G.: The Lagrangian particle dispersion model FLEXPART version 6.2, Atmos. Chem. Phys., 5(9), 2461–2474, 2005.

Stohl, A., Seibert, P., Arduini,J., Eckhardt, S., Fraser, P., Greally, B. R., Lunder, C., Maione, M., Mühle, J., O'Doherty ,S., Prinn, R. G., Reimann, S., Saito, T., Schmidbauer, N., Simmonds, P. G., Vollmer, M. K., Weiss, R. F., and Yokouchi, Y.: An analytical inversion method for determining regional and global emissions of greenhouse gases: Sensitivity studies and application to halocarbons, Atmos. Chem. and Phys. 9, 1597-1620, 2009.

Stohl, A., Kim, J., Li, S., O'Doherty, S., Mühle, J., Salameh, P. K., Saito, T., Vollmer, M. K., Wan, D., Weiss, R. F., Yao, B., Yokouchi, Y., and Zhou, L. X.: Hydrochlorofluorocarbon and hydrofluorocarbon emissions in East Asia determined by inverse modelling, Atmos. Chem. and Phys., 10, 3545-3560, 2010.

Sturrock, G. A., Etheridge, D. M., Trudinger, C. M., Fraser P. J., Smith A. M.: Atmospheric histories of halocarbons from analysis of Antarctic firn air: Major Montreal Protocol species, J. Geophys. Res., 107, D24, 4765, doi:10.1029/2002JD002548, 2002.

UNEP, Report on Emissions Reductions and Phase-Out of CTC (Decision 55/ 45), UNEP/OzL.Pro/ExCom/58/50, United Nations Environment Programme, Executive Committee of the Multilateral Fund for the Implementation of the Montreal Protocol: Montreal, 2009.

UNEP, Report of the UNEP Technology and Economic Assessment Panel: May 2013 Progress Report, Vol. 1, Kuijpers, L. and Seki M. (Eds.), United Nations Environment Programme, Nairobi,

Kenya (http://ozone.unep.org/Assessment_Panels/TEAP/Reports/TEAP_Reports/TEAP_Progress_Report_May_2013.pdf), 2013.

Vollmer, M. K., Zhou, L. X. , Greally, B. R., Henne, S., Yao, B., Reimann, S., Stordal, F., Cunnold, D. M., Zhang, X. C., Maione, M., Zhang, F., Huang, J., Simmonds, P. G.: Emissions of ozone-depleting halocarbons from China. Geophys. Res. Lett., 36, L15823, doi:10.1029/2009GL038659, 2009.

Walker, S. J., Weiss, R. F., Salameh P. K.: Reconstructed histories of the annual mean atmospheric mole fractions for the halocarbons CFC-11, CFC-12, CFC-113, and carbon tetrachloride, J. Geophys. Res., 105/C6, 14,285-14,296, 2000.

Weiss, R.F. and Prinn, R.G.: Quantifying greenhouse-gas emissions from atmospheric measurements: a critical reality check for climate legislation, Phil. Trans. R. Soc. A, 369, 1925-1942, doi:10.1098/rsta.2011.0006, 2011.

Yvon-Lewis, S. A. and Butler J. H.: Effect of oceanic uptake on atmospheric lifetimes of selected trace gases, J. Geophys. Res., 107(D20), 4414, doi:10.1029/2001JD001267,2002.

Xiao, X., Prinn, R. G., Fraser, P. J., Weiss, R. F., Simmonds, P. G., O'Doherty, S., Miller, B. R., Salameh, P. K., Harth, C. M., Krummel, P. B., Golombek, A., Porter, L. W., Butler, J. H., Elkins, J. W., Dutton, G. S., Hall, B. D., Steele, L. P., Wang, R. H. J., and Cunnold, D. M.: Atmospheric three-dimensional inverse modelling of regional industrial emissions and global oceanic uptake of carbon tetrachloride, Atmos. Chem. Phys., 10, 10421-10434, doi: 10.5194/acp-10-10421-2010, 2010.

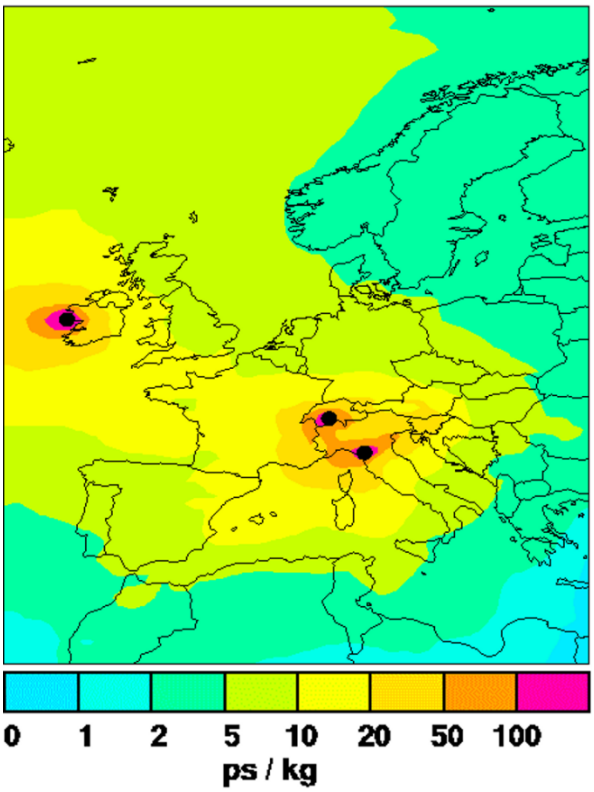


**Figure 1. Footprint emission sensitivity in picoseconds per kilogram (ps $kg^{-1}$) obtained from FLEXPART 20 days backward calculations averaged over all model calculations over two years (Jan 2008- Dec 2009). Measurement sites are marked with black dots.**

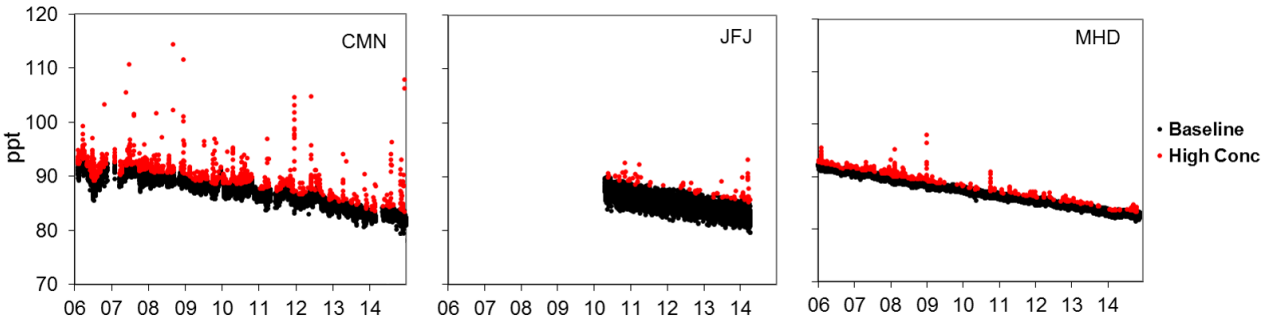


**Figure 2. $CCl_4$ time series at three European sites. Black dots: baseline, red dots: enhancements above the baseline.**

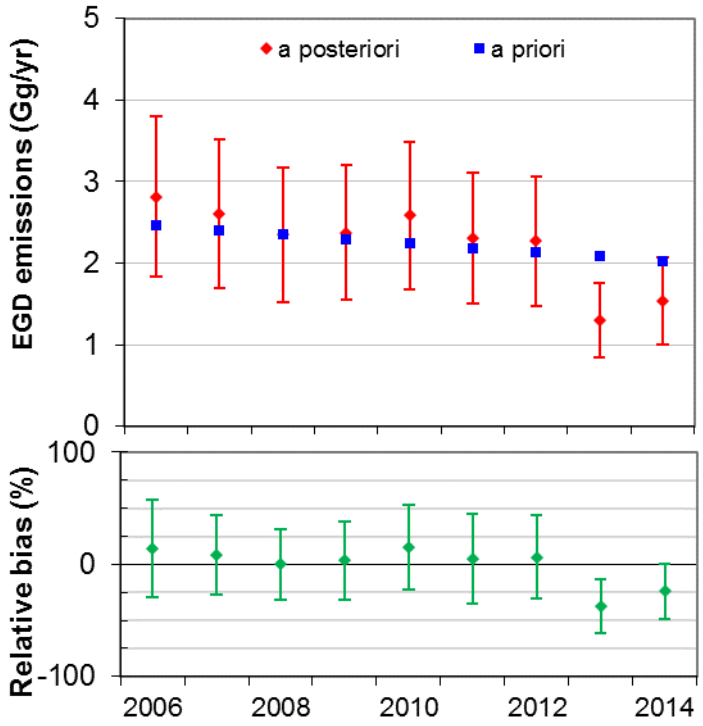


585 **Figure 3. Upper panel: comparison between the *a priori* (blue squares) and *a posteriori* (red diamonds) $CCl_4$ emission fluxes from the European Geographic Domain during 2006-2014. Bottom panel, percentage relative bias between the *a priori* and *a posteriori* time series (green diamonds).**

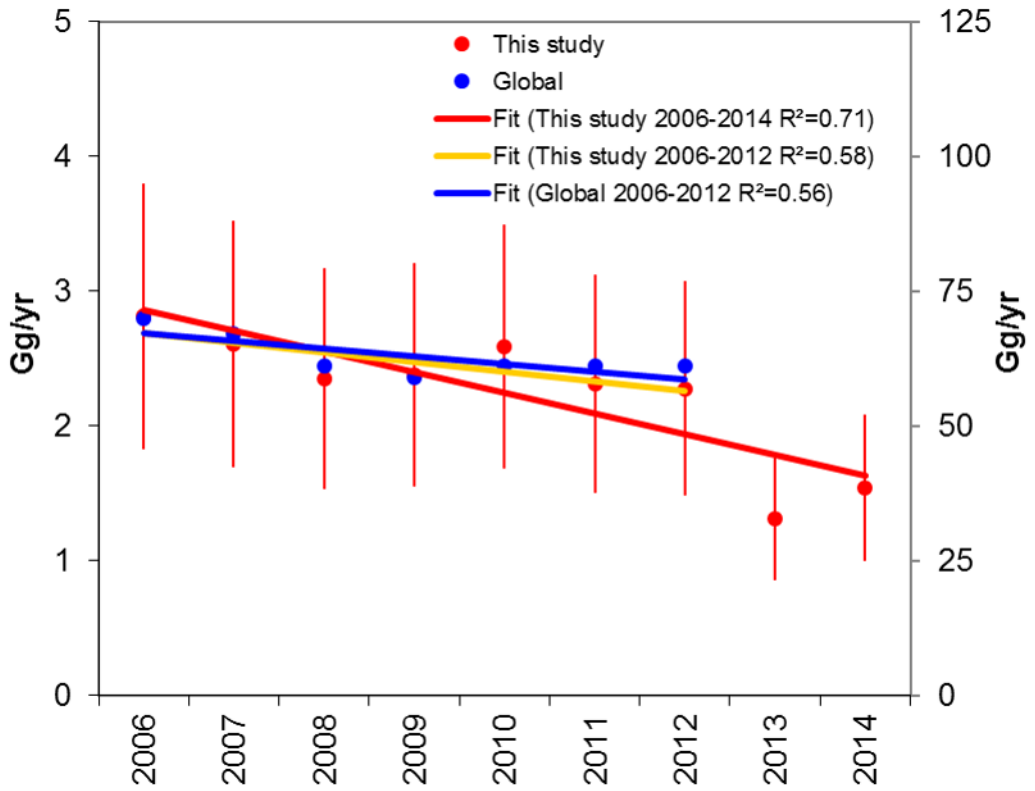


**Figure 4. European Geographic Domain $CCl_4$ emission fluxes derived in this study (red dots, left axis) compared with the global ones reported in Carpenter and Reimann et al. (2014) (blue dots, right axis). The red line represents the linear regression of our estimates over 2006 to 2014 (-6.9% $yr^{-1}$). Orange line: as for red lines but over 2006-2012 (-2.9 % $yr^{-1}$). Blue line: linear regression of global fluxes over 2006-2012 (-2.2 % $yr^{-1}$).**

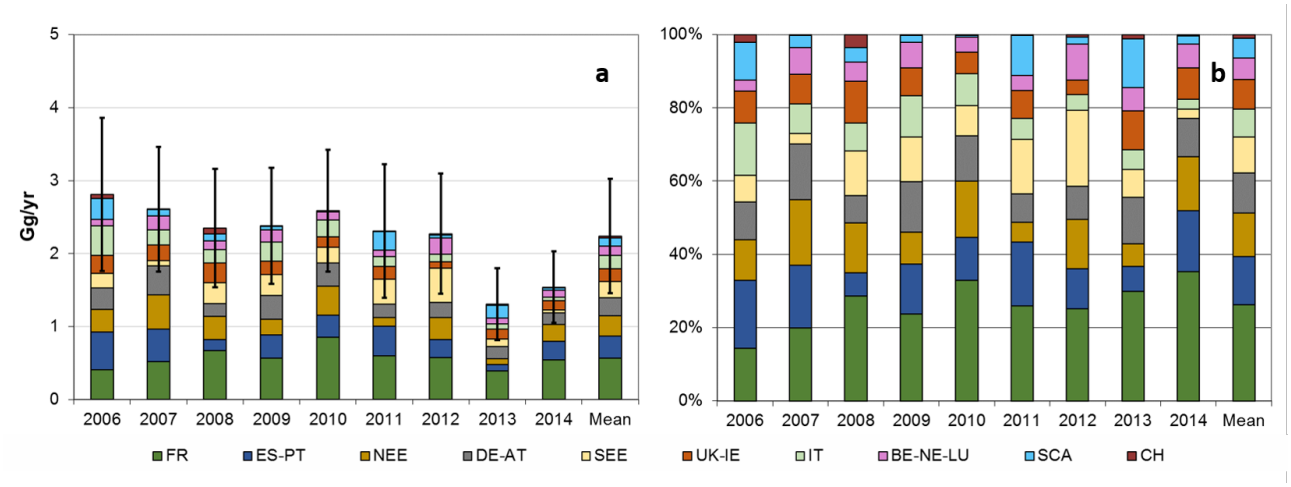


605

**Figure 5. a) Carbon tetrachloride estimated emission over the study period given in Gg $yr^{-1}$ from ten macro areas in the EGD. Error bars represent the uncertainty in emissions as derived by the inversion routine (see Supplementary Material) b) Yearly percent contribution of the single areas to total EGD emissions.**

610

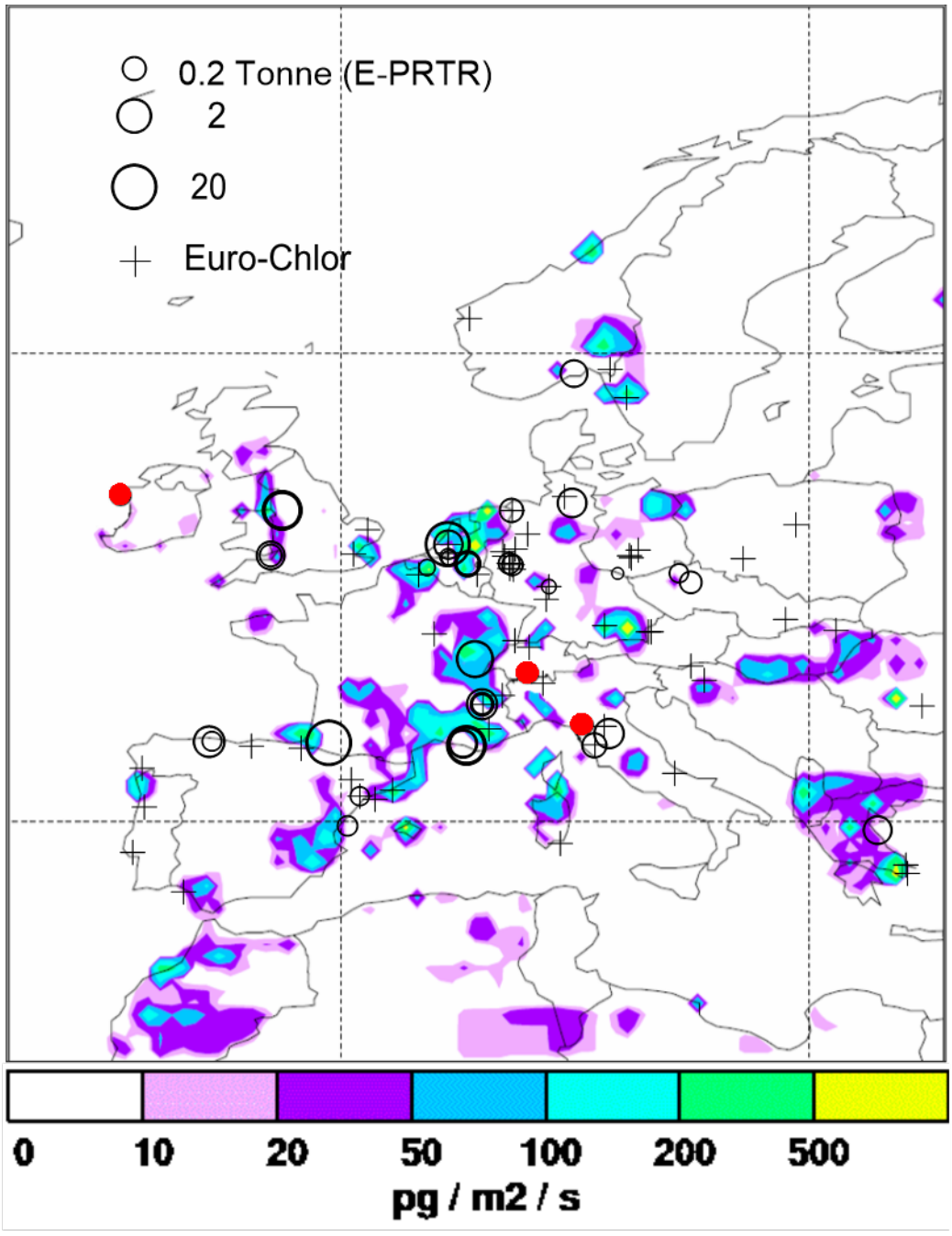


615

**Figure 6: Average *a posteriori* distribution of $CCl_4$ emissions from the European Geographic Domain over the study period. Measurement stations are marked with red dots. Open circles represent emissions to atmosphere as reported by the E-PRTR inventory and crosses correspond to the location of chlor-alkali plants listed in Eurochlor.**

620

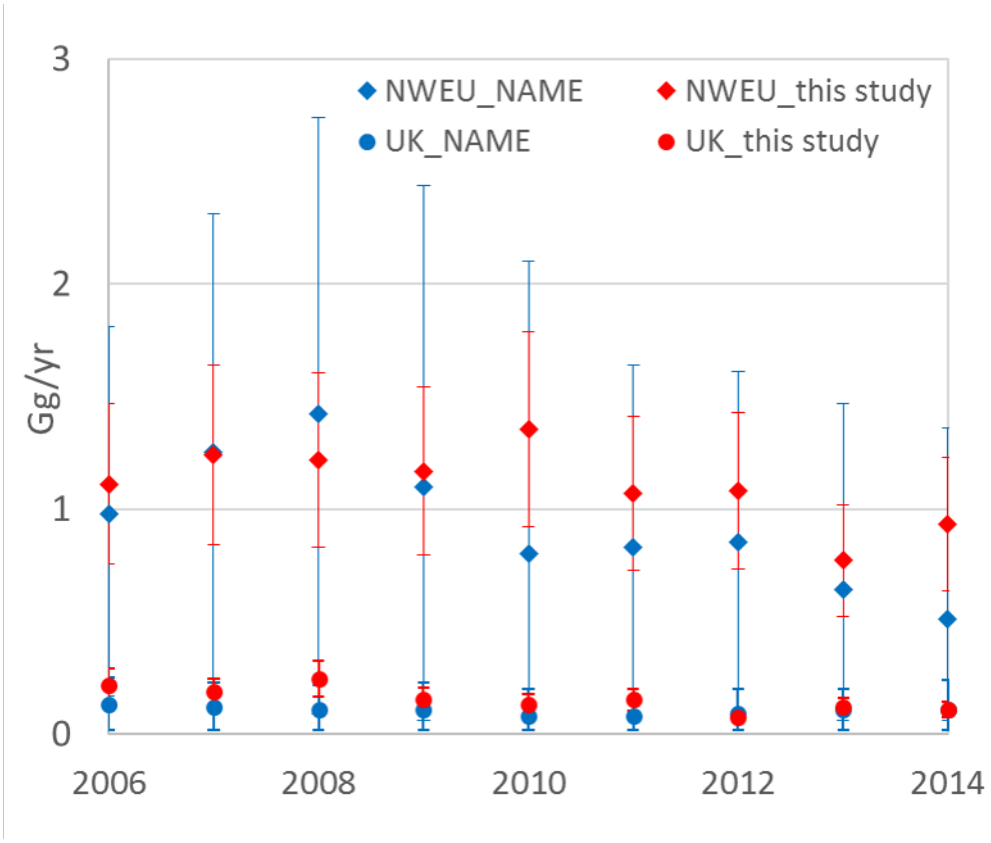


625

**Figure 7. Comparison between emissions from UK (circles) and the NWEU domain (diamonds) estimated through the NAME (blue) and the Bayesian (red) approach.**

630

**Table 1: Carbon tetrachloride emission estimates (Gg $yr^{-1}$) and associated uncertainty, percent yearly emission trends and 9-yr average percent contribution from the EGD and from ten macro areas in the EGD over the study period. Macro areas, listed according to their** 635 **emission intensity are: FR (France); ES-PT (Spain, Portugal); NEE (Poland, Czech Republic, Slovakia, Lithuania, Latvia, Estonia, Hungary, Romania, Bulgaria); UK-IE (United Kingdom, Republic of Ireland); DE-AT (Germany, Austria); IT (Italy); SCA (Norway, Sweden, Finland, Denmark); SEE (Slovenia, Croatia, Serbia, Bosnia-Herzegovina, Montenegro, Albania, Greece); BE-NE-LUX (Belgium, The Netherlands, Luxembourg), CH (Switzerland).**

640

| | $CCl_4$ yearly emissions (Mg yr-1) | | | | | | | | | | |
|---|---|---|---|---|---|---|---|---|---|---|---|
| Areas | 2006 | 2007 | 2008 | 2009 | 2010 | 2011 | 2012 | 2013 | 2014 | Trend %yr-1 | Mean |
| EGD | 2812±1058 | 2606±853 | 2348±807 | 2376±800 | 2586±837 | 2308±913 | 2272±822 | 1305±488 | 1538±485 | -6.9 | |
| FR | 405±109 | 519±140 | 671±181 | 563±152 | 849±229 | 597±161 | 572±154 | 391±106 | 542±146 | 0.0 | 26.2 |
| ES-PT | 519±189 | 444±162 | 151±55 | 323±118 | 303±110 | 405±148 | 248±90 | 87±32 | 257±94 | -10.1 | 13.2 |
| NEE | 311±118 | 468±177 | 318±120 | 209±79 | 399±151 | 123±47 | 305±115 | 81±31 | 226±86 | -9.9 | 11.8 |
| DE-AT | 290±81 | 396±110 | 176±49 | 327±91 | 319±89 | 181±50 | 206±57 | 166±46 | 161±45 | -8.7 | 11.0 |
| SEE | 205±120 | 76±45 | 286±168 | 291±171 | 213±125 | 342±201 | 471±277 | 100±59 | 38±22 | -1.3 | 9.8 |
| UK-IE | 241±60 | 212±53 | 269±67 | 181±45 | 149±37 | 175±44 | 88±22 | 138±35 | 132±33 | -9.7 | 8.0 |
| IT | 405±117 | 208±60 | 179±52 | 265±77 | 228±66 | 131±38 | 98±28 | 70±20 | 43±12 | -19.9 | 7.6 |
| BE-NE-LUX | 88±15 | 189±32 | 121±20 | 167±28 | 109±18 | 95±16 | 224±38 | 82±14 | 98±16 | -1.9 | 5.9 |
| SCA | 287±236 | 88±72 | 95±78 | 46±38 | 11±9 | 252±207 | 44±36 | 175±144 | 35±29 | -9.3 | 5.4 |
| CH | 61±12 | 6±1 | 82±16 | 4±1 | 6±1 | 7±1 | 16±3 | 15±3 | 6±1 | -23.8 | 1.0 |

# Supplementary material to Emissions of Carbon Tetrachloride (CCl4) from Europe

## Dispersion model

We run the Lagrangian particle dispersion model FLEXPART v-9.02 (Stohl et al., 1998, 2005; http://www.flexpart.eu) releasing every three hours, from all measurement sites, 40 000 particles followed backward in time for 20 days. This in order to calculate the emission sensitivity footprint also called source-receptor-relationship (SRR). The SRR describes the relationship between the contribution of potential sources at the receptor and the change in mixing ratios at the measurement site. Fig.1S shows the SRR for the three single stations, highlighting how the two continental stations (CMN and JFJ) are influenced by air masses originating in central Europe, whereas MHD is predominately influenced by Atlantic/Arctic air masses.

Fig. 2S shows the yearly (2012) emissions sensitivity produced using the three measurement sites. We observe a good SRR in the whole European Geographic Domain (EGD), with the exception of a small region in the Aegean area.

All the simulations are driven by European Centre for Medium-range Weather Forecast wind fields using 3-hourly ERA-Interim reanalyses (analysis fields at 00:00, 06:00, 12:00 and 18:00 UTC, and 3-h forecasts at 03:00, 09:00, 15:00 and 21:00 UTC were used) with 1°x1° horizontal resolution and 91 vertical levels.

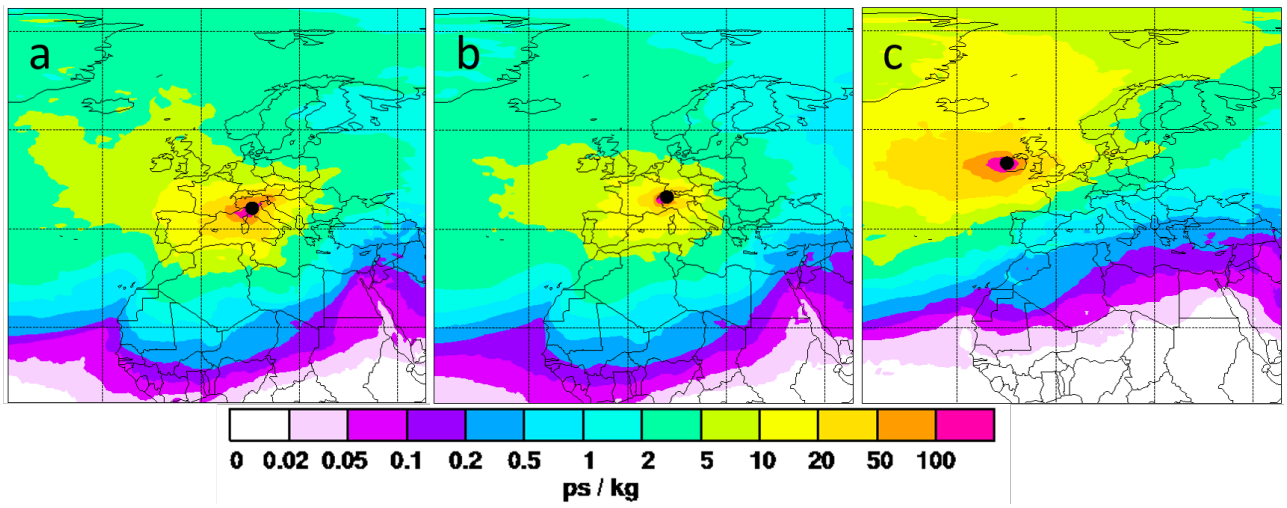


**Figure 1S. Single station SRR maps expressed in picoseconds per kilogram (ps $kg^{-1}$) obtained from FLEXPART 20 days backward calculations averaged over year 2012. Measurement sites are marked with black dots.**

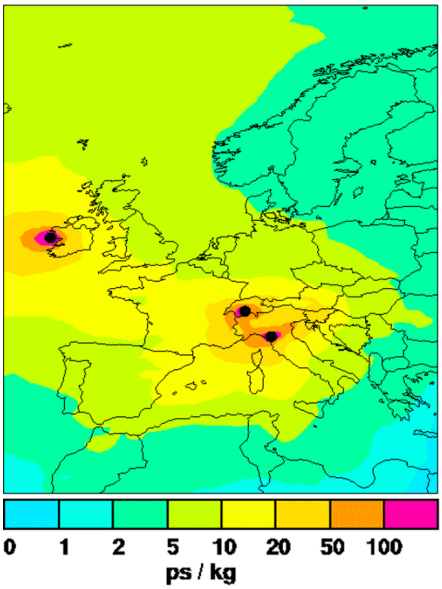


**Figure 2S. As in Figure 1S, but for the three stations.**

## Inversion method

To estimate the emissions of $CCl_4$ from the EGD we used the inversion method, based on a Bayesian optimization technique, described by Stohl et al. (2009, 2010), where all mathematical details can be found. The emission distribution and intensity found by the inversion represent the best fit between observation data and model simulation. Using a limited number of stations not all regions are well constrained by the observations, making the problem ill-conditioned and unstable. Therefore, to get the solution to our problem, we used an a priori gridded field of emission distribution and the associated uncertainty (Stohl et al., 2009; 2010).
The cost function to be minimized is:

$$1)\quad J = (M\tilde{x} - \tilde{y})^T diag(\sigma_0^{-2})(M\tilde{x} - \tilde{y}) + \tilde{x}^T diag(\sigma_x^{-2})\tilde{x}$$

Where the matrix *M* contains the model sensitivity, in our case all simulations produced by 40.000 particles run in backward mode for 20 days; the term $\tilde{x}$ represents the difference between the *a posteriori* and *a priori* emission vectors; $\tilde{y}$ is the difference between the observations and *a priori* simulated mixing ratios, $\sigma_0^{-2}$ is the vector of the standard error of observations, and $\sigma_x^{-2}$ is the *a priori* standard error vector.
Overall, the Bayesian inversion minimizes the cost-function reducing the model-observation misfit, represented by the first term on the right side of equation 1, optimizing the deviation of the solution from *a priori* emissions and its uncertainty, expressed by the second term of equation 1.

## Uncertainty evaluation

We associate for every grid cell an uncertainty value, $\sigma_x^j$

$$2)\quad \sigma^{j}_{x\_priori} = p * \max\left(k * x_j; l * x_{surf}\right)$$

Where $p$ is an appropriate uncertainty scaling factor; $x_j$ the *a priori* emission value in grid $j$; $x_{surf}$ the average land surface emissions flux; $k$ and $l$ are scaling factors set at 0.5 and 1, respectively (Keller et al., 2011; Fang et al., 2014; Maione et al., 2014). The last term on the right side of equation 2 allows associating large uncertainty values even to low emission grid cells. We tested several uncertainty scaling factors $p$ in order to optimise the agreement between modelled and observed mixing ratios. The increase of the uncertainty scaling factor $p$ yields a higher variability of the *a posteriori* flux from the single grid cells, leading to a decreasing root mean square (RMS) and increasing correlation coefficients between modelled and observed mixing ratios in all the three stations. However, for $p$ values larger than 6, new hotspots emerge in the *a posteriori* emission field with unrealistically large emissions from low sensitivity regions. We used $p$ = 2, a value giving higher correlation coefficients and lower RMS values. Noteworthy, differences in the EGD emissions lower than 5 % are obtained using $p$ values ranging between 1.5 and 4. The minimisation of the cost function reduces the *a priori* sigma value $\sigma^{j}_{x\_priori}$ giving, for each inverted grid cell an uncertainty value $\sigma^{j}_{x\_posteriori}$. For the whole domain we obtained an average uncertainty $\sigma^{j}_{x\_posteriori}$≅33%, with a smaller uncertainty (≈20 %) in high sensitivity boxes close to the receptors (e.g., FR and UK) and a larger uncertainty (≈80 %) in low sensitivity regions far away from the receptors (e.g., Scandinavian region).

**E-PRTR and Eurochlor**

The *a priori* emission field used in this study makes use of the European Pollutant Release and Transfer Register (E-PRTR) (http://prtr.ec.europa.eu/) inventory and of the Eurochlor reports (http://www.eurochlor.org/).

*E-PRTR*

E-PRTR is the Europe-wide register that provides data from industrial facilities in European Union Member States and in Iceland, Liechtenstein, Norway, Serbia and Switzerland. It replaced and improved upon the previous European Pollutant Emission Register (EPER). The register contains data reported annually by more than 30,000 industrial facilities covering 65 economic activities across Europe. For each facility, information are provided concerning the amounts of pollutant releases to air, water and land as well as off-site transfers of waste and of pollutants in wastewater from a list of 91 key pollutants including $CCl_4$. Over the period 2007-2014, 37 $CCl_4$ emitting activities are reported. According to E-PRTR, the "industrial scale production of basic organic chemical" is the main $CCl_4$ declared source in the database, being responsible for the 93.9 % of total European emissions, as shown in Figure 3S reporting the percentage contribution to $CCl_4$ emissions from each industrial facility, averaged over 2007-2014.

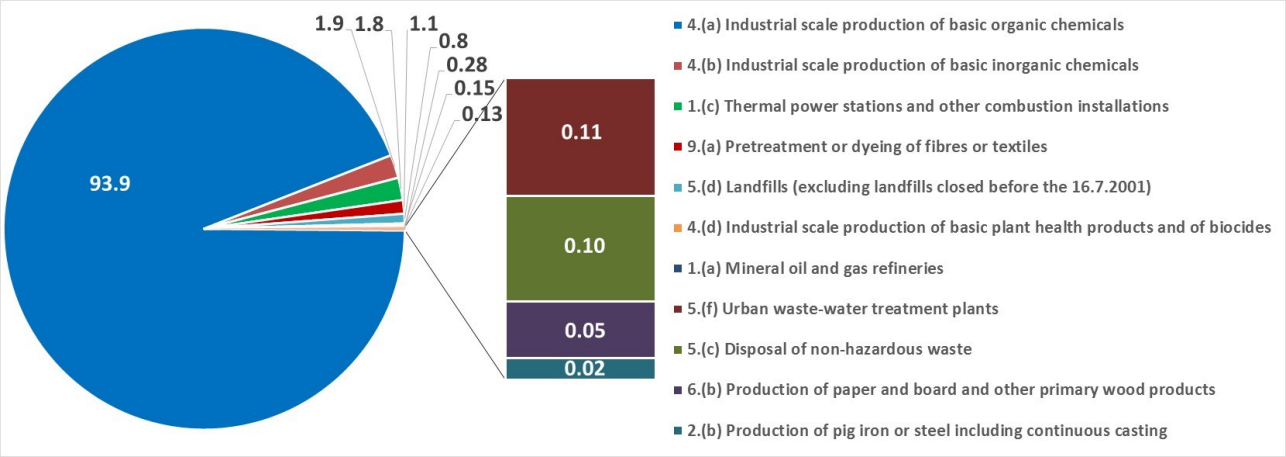


**Figure 3S. Average percentage contribution of different source sectors to the total $CCl_4$ emissions reported in the E-PRTR (2007-2014).**

Figure 4S shows the average percent contribution to the total $CCl_4$ flux for each macro area in the EGD over the period 2007-2014. FR alone results to be responsible for 65% of the emissions from the EGD, with an average emission of 0.02 Gg $yr^{-1}$. BE-NE-LUX and UK-IE follows with 13.5 and 11%, respectively. NEE, SCA and CH do not report any emission.

As reported in the paper main text (paragraph "Emission hot spots"), the inversion results estimate a $CCl_4$ emission flux much larger than that declared in the E-PRTR. For major detail, we report in Fig. 5S the percent ratio between emissions reported in the E-PRTR and our estimates for each macro-area in the domain during 2007-2014. The E-PRTR reported emissions from the EGD represent on average, over the considered period, 4 % of the emissions obtained through the inversion. Lower discrepancies are found for the BE-NE-LUX and FR macro areas where the declared emissions reach the 30 % and 21% of inversion estimation, respectively.

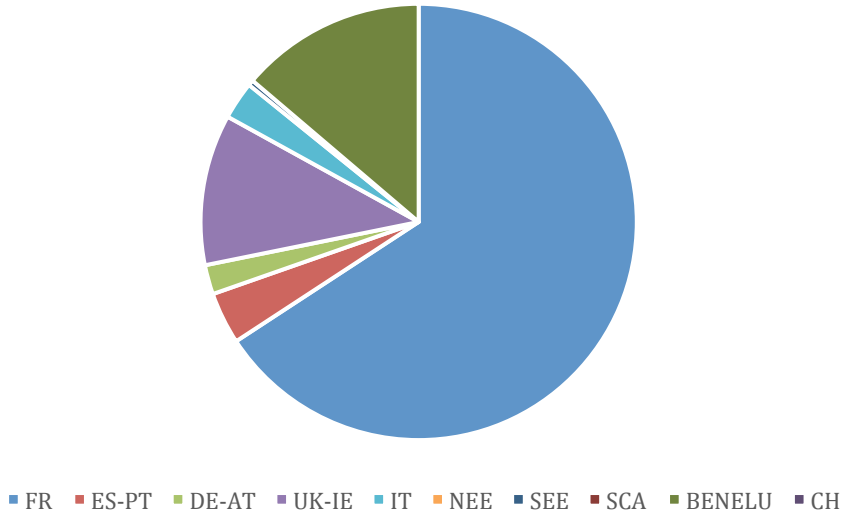


**Figure 4S. Average percent contribution to the total $CCl_4$ flux for each macro area in the EGD over the period 2007-2014.**

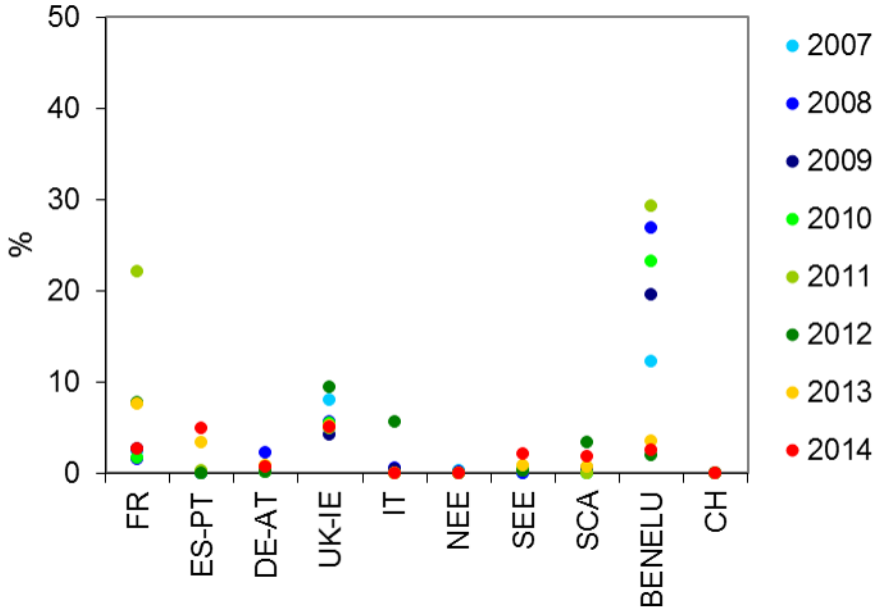


**Figure 5S. Percent ratio between emissions as in the E-PRTR and the inversion results for each macro-area in the domain during 2007-2014.**

*Chlorine industry in Europe: Eurochlor*

One of the main $CCl_4$ emission source is the chlor-alkali industry. Information on chlorine and chlorine derivatives production in Europe is given by Eurochlor, an association representing the 97% of chlorine production in Europe. The total number of plants reported by Eurochlor over the period 2006-2014 is 84 (of which 10 in common with the E-PRTR). Eurochlor releases annual reports where potential chlorine production for each industry is given, together with the adopted technology. However, Eurochlor reports do not include information on the $CCl_4$ emission factors according to the adopted technology. Since 1990's chlorine production in Europe is significantly changed. In 1997 ca 64% of the chlor-alkali industry was based on mercury cell technology and only 10% was based on the cleaner membrane cell process. Currently, the latest accounts by 60% against the 25% of the mercury technology. Over the same period the use of diaphragm cells was reduced from 22 to 12%, while other technologies represent only the 2-3% of the total. Further uncertainties could be due to the employment of $CCl_4$ in industrial processes where it is used as a process agent in the chlor-alkali plants for the elimination of nitrogen trichloride and the recovery of chlorine from tail gases. In Europe plants that are allowed to use directly $CCl_4$ (European Union, 2010) were only eight in 2010, of which three in France. However, this source is difficult to assess because the allowed facilities do not have any obligation to report the actual use of the allocated $CCl_4$ quota and/or the transfer of this quota to another plant. According to DG CLIMA (2012) in 2011 only three chlor-alkali plants in Europe were using $CCl_4$, and reported emissions ranged from 0 to 30 g $CCl_4$/tonne annual chlorine capacity, depending on the frequency of use and the occurrence of accidents (Brinkmann et al., 2014).

The graph in Figure 6.S reports the percent potential chlorine production for each macro area. The major contributor is the DE-AT macro area accounting for 40%, followed by BE-NE-LUX with 15.8%. FR, that according to the E-PRTR is responsible for the 65% of European $CCl_4$ emissions, is the third potential chlorine producer, accounting for the 12%.

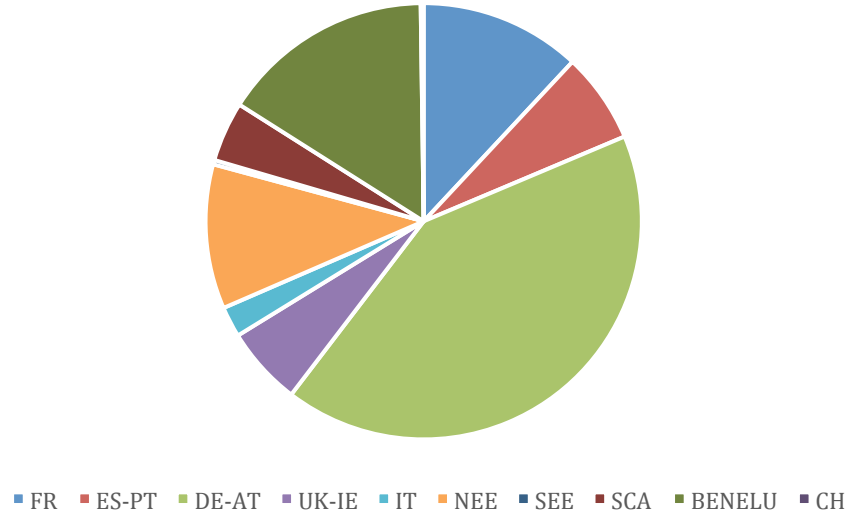


**Figure 6S. Percent potential chlorine production for each macro area in the EGD (Eurochlor, 2014).**

In Figure 7.S the percentages of adopted technologies in each macro area in the EGD are reported. It should be noted that in ES-PT, CH and NEE more than 50% of the production is still based on the mercury cell technology. In FR and DE-AT there is still a significant use of diaphragm cells. To be noted that within the DE-AT macro area, Eurochlor does not report any plant in Austria.

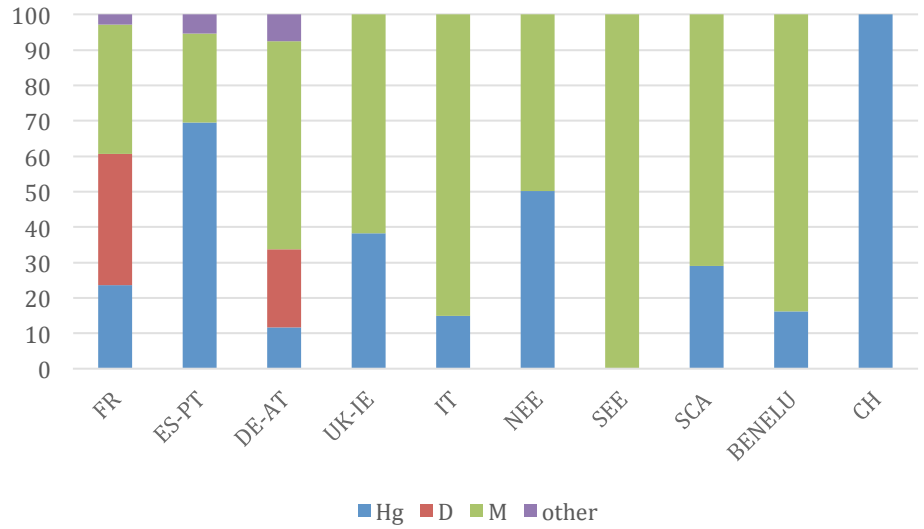


**Figure 7S. Percentages of adopted technologies in each macro area. Hg: mercury cell technology; D: diaphragm cell; M: membrane cell (Eurochlor, 2014).**

***A priori* emission field**

The construction of the *a priori* emission field is a challenging aspect of the methodology adopted in this study, since $CCl_4$ emission fluxes are affected by high uncertainty.

Possible $CCl_4$ emission sources are: chlor-alkali plants (UNEP, 2012); emissions produced by feedstock use; petrol-chemical, pesticide, and fire extinguisher industry (UNEP, 2006; 2012); methane chlorination, toxic waste treatment, landfills, incinerators (Fraser et al., 2014); and bleach containing domestic cleaning agents (Odabasi et al., 2008; 2014).

The latest have been evaluated up to 0.49 Gg $yr^{-1}$ for a population of 600 millions in the EGD and this amount has been distributed following the population (CIESIN, 2010) density in all the *a priori* emission fields tested in this work. The remaining non-diffuse emissions have been parameterised following six different ways (F1-F6).

A reference $CCl_4$ emission value for Europe is that given by Xiao et al. (2010), who estimated an average emission of 3.0 ± 1.6 Gg $yr^{-1}$ over 1996-2004. Since our tests have been performed for the year 2012, we applied to such average value a 2% decrease, following the projection given by Fraser et al. (2012), resulting in an emission from the EGD of 2.38 Gg $yr^{-1}$.

Here we give a detailed description of each *a priori* emission field tested: Please note that fluxes taken by Eurochlor and E-PRTR are always geo-referenced:

F1: 0.49 Gg $yr^{-1}$ distributed according to the population density; 1.89 Gg $yr^{-1}$ (i.e., the total estimated EGD emission of 2.38 Gg $yr^{-1}$ minus the 0.49 Gg $yr^{-1}$ diffuse emission) are attributed to the chloro-alkali plants evenly distributed among each single plant given in the E-PRTR and in the Eurochlor databases.

F2: 0.49 Gg $yr^{-1}$ distributed according to the population density; 1.89 Gg $yr^{-1}$ as follows: 50% of this flux is evenly distributed among each of the 37 plants listed in the E-PRTR and 50% evenly distributed among the Eurochlor plants (74); in this way F2 assigns a greater role to the E-PRTR plants.

F3: as for F2 but the 50% attributed to the E-PRTR plants is distributed according percent relative contribution to emissions declared by each plant (i.e., if a plant is declaring the 20% of the total $CCl_4$ reported in the E-PRTR, we assign to this plant the same percentage); similarly, for the Eurochlor plants the 50% is distributed according to the percent relative distribution of the declared chlorine production.

F4: the emissions declared in the E-PRTR, i.e. 0.064 Gg $yr^{-1}$ have been distributed among the single cells where plants are located (Eurochlor plants not included because no information about $CCl_4$ emissions is given by this database), while 2,32 Gg $yr^{-1}$ (i.e. the total estimated EGD emission of 2.38 Gg $yr^{-1}$ minus the 0.064 Gg $yr^{-1}$ E-PRT flux) are distributed according to the population density.

In addition, we have tested two *a priori* emission fields where the total EGD emission do not correspond to the 2.38 Gg $yr^{-1}$ derived from Xiao et al. (2010):

F5: 0.49 Gg $yr^{-1}$ distributed according to the population density; to such value a flux is added calculated applying an emission factor of 0.4 kg $CCl_4$ for each tonne of chlorine produced by all plants included in the Eurochlor database. Finally the $CCl_4$ emissions as declared in the E-PRTR are added. It should be noted that the *a priori* emission flux derived corresponds to 4.4 Gg $yr^{-1}$ for the EGD in 2012. The 0.4 kg $CCl_4$ for each tonne of chlorine produced emission factor has been suggested by Paul Fraser (personal communication).

F6: as in F5, but applying an emission factor of 0.03 kg $CCl_4$ for each tonne of chlorine produced by all plants (Brinkmann et al., 2014) included in the Eurochlor database. It should be noted that the *a priori* emission flux derived corresponds to 0.6 Gg $yr^{-1}$ for the EGD in 2012.

In order to evaluate the inversion performance for the various *a priori* emission fields tested, we compared i) the correlation values ($ra^2$) between the modelled and the observed concentration time obtained using the *a priori* emission fluxes F1÷F6; ii) the correlation values ($rb^2$) between the modelled and the observed concentration time obtained using the *a posteriori* emission fluxes F1÷F6. In Table 1S the $ra^2$ and $rb^2$ values for each station are reported as well as the emission flux produced by a given *a priori* emission field (F1÷F6) from the entire EGD. In all the reported tests, $rb^2$ values are always higher than $ra^2$ values, i.e. the *a posteriori* emission field gives account of a better representation of the variance of the measured signal with respect to the *a priori*. In addition, "EGD emission" *a posteriori* values obtained using quite different *a priori* emission fields are very similar (well within the error bar), confirming that the inversion is robust enough and converges towards a reliable emission estimate. In light of such results, we decided to use an "ensemble" *a priori* emission field, built as follows: to each macro area we assigned an emission flux given by the average, for that macro area, of the *a posteriori* emission fields produced by F1÷F6. The share given by diffuse emission has been distributed according to the population density, whereas the remaining share has been equally assigned (and geo-referenced) to each plant in that macro area. The "Ensemble" row in Table 1S reports the $ra^2$ and $rb^2$ values, as well as the obtained EGD emission flux. The "Ensemble" *a priori* emission field has been used for estimating $CCl_4$ emissions over the study period.

**Table 1S. Comparison among different *a priori* emission fields. F1÷F6 and "Ensemble" represent the *a priori* emission fields described in the text. $ra^2$: Correlation between modelled concentration fluxes obtained by a given *a priori* emission field and the observations at the three measurement sites. $rb^2$, as $ra^2$ but for the *a posteriori* emission fluxes. The tests have been performed for year 2012.**

| ***A priori* emission field** | **CMN** | | **JFJ** | | **MHD** | | **EGD emissions** |
|---|---|---|---|---|---|---|---|
| | $ra^2$ | $rb^2$ | $ra^2$ | $rb^2$ | $ra^2$ | $rb^2$ | Gg $yr^{-1}$ |
| F1 | 0.45 | 0.58 | 0.31 | 0.42 | 0.66 | 0.79 | 2.3 ± 0.8 |
| F2 | 0.45 | 0.58 | 0.29 | 0.39 | 0.66 | 0.79 | 2.1 ± 0.8 |
| F3 | 0.40 | 0.58 | 0.27 | 0.37 | 0.59 | 0.78 | 2.2 ± 0.8 |
| F4 | 0.48 | 0.58 | 0.35 | 0.44 | 0.70 | 0.78 | 2.1 ± 0.7 |
| F5 | 0.38 | 0.58 | 0.25 | 0.37 | 0.35 | 0.78 | 2.4 ± 0.9 |
| F6 | 0.49 | 0.58 | 0.32 | 0.42 | 0.74 | 0.79 | 2.1 ± 0.8 |
| | | | | | | | |
| Ensemble | 0.49 | 0.58 | 0.35 | 0.44 | 0.75 | 0.79 | 2.3 ± 0.8 |

**Subsets of data**

Because of the limited numbers and localisation of the receptors, the simulations cannot produce a homogeneous sensitivity over the study domain. In order to assess to what extent our results are sensitive to the receptors used, we run the inversions removing one station at a time

The EGD emissions obtained with different subsets of observation data are consistent with those obtained using the full set. The larger difference, 26 %, is registered when removing MHD. Removing JFJ and CMN, produced a similar percentage difference of -10 % and -9 %, respectively, as a consequence of the similar footprint of the two receptors. This result indicates the stability of the inversion system even when using a subset of data and reinforce the benefit of the increased sensitivity over domain when using an increasing number of receptors.

**Model performance at the stations**

With the aim of evaluating the model performance and the station specific errors, we compared the observed and modelled time series at the three stations, taking into account different statistical parameters, in a similar way as described in Stohl et al. (2009), Maione et al. (2014) and Graziosi et al. (2015). The results of this comparison, carried out for the year 2012, are reported in Table 2S.
$1 - E_b/E_a$ is the relative error reduction, where $E_a$ and $E_b$ are the *a priori* and *a posteriori* RMS errors. The values achieved at the stations used in this study are in a range between 16 % and 23 %, in spite of the different station characteristics.
The Pearson correlation coefficients described in the following show a better performance for MHD because of the poorer model performance in the mountain area. However, as stated in Mahowald et al. (1997), using receptors closer to the main source regions would improve the model performance to acquire source information.
$r_a^2$ is the squared Pearson correlation coefficients between the time series obtained at receptor using the *a priori* emission field and the observed time series, and $r_b^2$ between the *a posteriori* and observed time series. These coefficients are used to evaluate the proximity of the modelled emission field to the real one. The obtained $r_b^2$ values higher than $r_a^2$ are an indication of the improvement of the *a posteriori* emission field with respect to the *a priori*.
Analogously to $r_a^2$ and $r_b^2$, the squared Pearson correlation coefficients $r_{ba}^2$ (and $r_{bb}^2$) between the modelled *a priori* (and *a posteriori*) and the measured baseline mixing ratios at the three stations indicate the capability of the system to reproduce the variability and trends of the baseline.
Transport events from the source regions to the receptors generate the variability in the observed enhancements above the baseline. The correlation analyses between the observed and simulated *a priori* ($r_{ea}^2$) and the *a posteriori* ($r_{eb}^2$) polluted mixing ratios describe the system capability to reproduce concentrations above the background. Higher correlation values are obtained at the remote station of MHD. Despite the relatively low $r_{ea}^2$ and $r_{eb}^2$ values at CMN and JFJ, data from these two mountain stations improve the inversions on the regional scale, thanks to the station sensitivity to the main source regions. For the same reason, the two mountain stations also present higher standard deviation (SD) of the observed mixing ratios.

**Table 2S. Station parameters. Mean, mean CCl4 mixing ratios; SD, standard deviation of the observed mixing ratios; N, number of observations; $E_a$, RMS *a priori* error; $E_b$, RMS *a posteriori* error; $1-E_a/E_b$, relative error reduction; $r^2_a$ and $r^2_b$, squared Pearson correlation coefficients between the observations and the *a priori* ($r^2_a$) and *a posteriori* ($r^2_b$) simulated time series; $r^2_{ba}$ (and $r^2_{bb}$) is the squared Pearson correlation coefficients between the *a priori* (and *a posteriori*) baseline and the measured concentrations; $r^2_{ea}$ (and $r^2_{eb}$) is the squared Pearson correlation coefficients between the *a priori* (and *a posteriori*) enhancements above the baseline and the measured concentrations.**

| Station | Mean (ppt) | SD (ppt) | N | $E_a$ (ppt) | $E_b$ (ppt) | $1-E_b/E_a$ | $r^2_a$ | $r^2_b$ | $r^2_{ba}$ | $r^2_{bb}$ | $r^2_{ea}$ | $r^2_{eb}$ |
|---|---|---|---|---|---|---|---|---|---|---|---|---|
| CMN | 85.7 | 1.1 | 2039 | 0.82 | 0.64 | 0.23 | 0.48 | 0.58 | 0.53 | 0.55 | 0.24 | 0.33 |
| JFJ | 84.7 | 0.8 | 2124 | 1.12 | 0.94 | 0.16 | 0.35 | 0.44 | 0.24 | 0.26 | 0.19 | 0.22 |
| MHD | 84.9 | 0.3 | 2833 | 0.64 | 0.50 | 0.23 | 0.75 | 0.79 | 0.75 | 0.76 | 0.55 | 0.63 |

## References


Brinkmann, T., Giner Santonja, G., Schorcht, F., Roudier, S., Delgado Sancho, L.: Industrial Emissions Directive 2010/75/EU, Integrated Pollution Prevention and Control, Science and Policy Reports. Best Available Techniques (BAT). Reference Document for the Production of Chlor-alkali. EC-JRC, Joint Research Centre of the European Commission, Luxembourg: Publications Office of the European Union, 2014.

CIESIN, Center for International Earth Science Information Network (CIESIN): Gridded Population of the World: Future Estimates, Socioeconomic Data and Applications Center (SEDAC), Columbia University, Palisades, NY, USA, 2010. Available at http://sedac.ciesin.columbia.edu/gpw.

EC DG CLIMA (European Commission, Directorate General Climate Action), Report of undertakings on consumption and emissions of controlled substances as process agents under regulation EC/1005/2009, 2012.

European Union, Commission Decision of 18 June 2010 on the use of controlled substances as process agents under Article 8(4) of Regulation (EC) No 1005/2009 of the European Parliament and of the Council, 2010/372/EU, 2010.

Fang X. K., Thompson R. L., Saito T., Yokouchi Y., Kim J., Li S., Kim K. R., Park S., Graziosi F., Stohl, A.: Sulfur hexafluoride (SF6) emissions in East Asia determined by inverse modelling, Atmos. Chem. Phys., 14, 4779-4791, 2014.

Fraser, P., Dunse, B., Manning, A. J., Wang, R., Krummel, P., Steele, P., Porter, L., Allison, C., O'Doherty, S., Simmonds, P., Mühle, J., and Prinn, R.: Australian carbon tetrachloride (CCl4) emissions in a global context, Environ. Chem., 11, 77–88, 2014.

Graziosi, F., Arduini, J., Furlani, F., Giostra, U., Kuijpers, L. J. M., Montzka, S. A., Miller, B. R., O'Doherty, S. J., Stohl, A., Bonasoni, P., and Maione, M.: European emissions of HCFC-22 based on eleven years of high frequency atmospheric measurements and a Bayesian inversion method, Atmos. Environ., 112, 196, 2015.

Keller, C. A., Brunner, D., Henne, S., Vollmer, M. K., O'Doherty, S., and Reimann, S.: Evidence for under-reported western European emissions of the potent greenhouse gas HFC-23, Geophys. Res. Lett., 38, L15808, doi:10.1029/2011gl047976, 2011.

Mahowald, N. M., Prinn, R. G., and Rasch, P. J.: Deducing $CCl_3F$ emissions using an inverse method and chemical transport models with assimilated winds, J. Geophys. Res., 102, 28153–28168, 1997.

Maione M., Graziosi, F., Arduini, J., Furlani, F., Giostra, U., Blake, D.R., Bonasoni, P., Fang, X., Montzka, S.A., O'Doherty, S.J., Reimann, S., Stohl, A., and Vollmer, M.K.: Estimates of European emissions of methyl chloroform using a Bayesian inversion method, Atmos. Chem. and Phys. 14, 9755-9770, doi:10.5194/acp-14-9755-2014, 2014.

Odabasi M.: Halogenated volatile organic compounds from the use of chlorine-bleach containing household products, Environ. Sci. and Technol. 42, 1445-1451, 2008.

Odabasi M., Elbir T., Dumanoglu Y., & Sofuoglu SC.: Halogenated volatile organic compounds in chlorine-bleach-containing household products and implications for their use, Atmos. Environ., 92, 376-383, 2014.

Stohl, A., Hittenberger, M., and Wotawa, G.: Validation of the Lagrangian particle dispersion model FLEXPART against large scale tracer experiment data, Atmos. Environ., 32, 4245–4264, 1998.

Stohl, A., Forster, C., Frank, A., Seibert, P., and Wotawa, G.: The Lagrangian particle dispersion model FLEXPART version 6.2, Atmos. Chem. Phys., 5(9), 2461–2474, 2005.

Stohl, A., Seibert, P., Arduini,J., Eckhardt, S., Fraser, P., Greally, B. R., Lunder, C., Maione, M., Mühle, J., O'Doherty ,S., Prinn, R. G., Reimann, S., Saito, T., Schmidbauer, N., Simmonds, P. G., Vollmer, M. K., Weiss, R. F., and Yokouchi, Y.: An analytical inversion method for determining regional and global emissions of greenhouse gases: Sensitivity studies and application to halocarbons, Atmos. Chem. and Phys. 9, 1597-1620, 2009.

UNEP/CTOC, United Nations Environment Programme/Chemicals Technical Options Committee, 2006. Report of the Chemicals Technical Options Committee (Nairobi, Kenya).

UNEP/TEAP, United Nations Environment Programme/Technology and Economic Assessment Panel, 2012. Report on the Technology and Economic Assessment Panel (Nairobi, Kenya).

Xiao, X., Prinn, R. G., Fraser, P. J., Weiss, R. F., Simmonds, P. G., O'Doherty, S., Miller, B. R., Salameh, P. K., Harth, C. M., Krummel, P. B., Golombek, A., Porter, L. W., Butler, J. H., Elkins, J. W., Dutton, G. S., Hall, B. D., Steele, L. P., Wang, R. H. J., and Cunnold, D. M.: Atmospheric three-dimensional inverse modelling of regional industrial emissions and global oceanic uptake of carbon tetrachloride, Atmos. Chem. Phys., 10, 10421-10434, doi: 10.5194/acp-10-10421-2010, 2010.